WORLD JOURNAL OF PHARMACEUTICAL RESEARCH
Coden USA: WJPRAP Impact Factor 8.453
Volume 15, Issue 3, 1210-1227. Research Article ISSN 2277–7105

RESPONSE SURFACE MODELLING FOR THE EFFICIENT PHOTODEGRADATION OF 2, 4-DICHLOROPHENOXYACETICACID USING SILVER NANOPARTICLES

Sheena Sreejan Anuvrinda[1], Rajashekara Rakshitha[1], Nagaraju Pallavi[1]*

[1]Department of Environmental Science, School of Life Sciences, JSS Academy of Higher Education and Research, Mysuru- 570015, India.

Article Received on 31 Dec. 2025,
Article Revised on 22 Jan. 2026,
Article Published on 01 Feb. 2026

https://zenodo.org/records/18438379

***Corresponding Author**

Nagaraju Pallavi

Department of Environmental Science, School of Life Sciences, JSS Academy of Higher Education and Research, Mysuru- 570015, India.
anupallavi@jssuni.edu.in

How to cite this Article: Sheena Sreejan Anuvrinda[1], Rajashekara Rakshitha[1], Nagaraju Pallavi[1]*. (2026). Response Surface Modelling For The Efficient Photodegradation of 2, 4-Dichlorophenoxyaceticacid Using Silver Nanoparticles. World Journal of Pharmaceutical Research, 15(3), 1210–1227.

ABSTRACT

2,4-Dichlorophenoxyacetic acid (2,4-D) is one of the most widely used herbicides. As a result, the aquatic environment and human health are threatened by its residue. In order to examine and compare how 2,4-Dichlorophenoxyacetic acid degrades under artificial and natural light, Ag was successfully synthesized from Azadirachta indica (Neem) extract at room temperature via co precipitation method. Response Surface Modelling, which is a statistical tool used in the current work to optimise processes like photo catalysis with the least amount of laboratory analysis. Field emission scanning electron microscopy, X- Ray diffraction, Fourier transforms infrared spectrometry, Energy dispersive X-ray spectroscopy, were some of the characterization techniques used. The characterization of Ag nanoparticles confirmed the formation of crystalline structure and reviled that few parameters, including reactant concentration, reactant mixing ratio, reactant interaction time, etc., had a significant impact on the morphology and size of the nanoparticles. This work shows that 2, 4-D would be removed at a constant rate throughout the photo catalytic reaction (R^2> 0.99). The highest percentage of 2,4-D herbicide 93.4% was efficiently degraded by the photo catalytic activity of Ag nanoparticles. (15 mg catalyst; 10 ppm 2,4-D concentration). Sunlight showed a higher percentage of degradation as compared to artificial light. In view of this, it can be stated that Ag is a material with great potential for 2,4-D photo catalytic degradation under optimal conditions.

KEYWORDS: Neem extract, Photocatalytic degradation, Synthesis, Response Surface Modelling, Silver nanoparticles.

1. INTRODUCTION

The nanoparticles have physical, chemical, and biological characteristics that are different from those of the bulk materials.[1] Silver and gold nanoparticles among the different inorganic nanoparticles offer exceptional material qualities and functional diversity.[2] The uses of nano silver are numerous and significant. They are extensively utilised in photonics, microelectronics, photocatalysis, and antimicrobial processes.[3],[4] A developing area of nanoscience during the past decade is the green synthesis of nanomaterials using various plant resources.[5]

Nanoparticles were previously synthesised using physical and chemical processes.[6] There are numerous drawbacks to chemical and physical approaches. Physical methods need a lot of energy and money; Chemical synthesis uses potentially harmful substances for the environment.[7] Due to the increased demand for ecologically friendly material synthesis technologies, biosynthesis of nanoparticles has drawn a lot of attention.[8] Biological methods of nanoparticle production involving microbes, enzymes, and plants or plant extracts have been developed as potential sustainable alternatives for chemical and physical processes.[9] Due to the simplicity of synthesis, ecological sustainability, and increased stability of nanoparticles, bio reduction approaches based on fungi, microbes, and plant extracts are currently being studied.[10,11]

The use of plant-based extracts to make AgNPs has become more popular.[11] For the production of nanoparticles, plant extracts serve as reducing and capping agents.[12] AgNPs' capping prevents nanoparticle agglomeration, lowers toxicity, and boosts antibacterial activity.[13] Due to the simplicity of scaling up, the biohazards, and the complex process of maintaining cell cultures, using plant extracts for synthesis of nanoparticles may be more preferable compared to the use of microorganisms.[14][15] In this context, neem leaf extract from the Meliaceae family plant (Azadirachta indica) was employed in order to convert silver ions to nanoparticles.[16] Neem leaves extract was chosen for the current study because; (i) It does not require the addition of an external stabilising agent during synthesis(ii) It offers synergistic effects to enhance the antimicrobial properties of the synthesised silver nanoparticles (one of the major ends uses), and(iii) It has been shown to be non-pathogenic.[17] The goal of this work was to assess the idea of environmentally friendly

synthesis of AgNPs using plant extract and to create a modified method for producing AgNPs at room temperature without the use of hazardous or toxic substances.[18,19]

The generated particles were identified as silver nanoparticles by UV spectroscopic examination. The production of crystalline silver nanoparticles was confirmed by the X-ray diffraction analysis. The FESEMs showed that process variables such reluctant concentrations, mixing ratio of the reactants, and reactant interaction duration greatly influenced the morphology and size of the nanoparticles.

Environmental contamination is a result of how rapidly human society has progressed and developed. In the case of the agricultural industry, cropland has been treated with herbicides to restrict the growth of seeds.[19] In order to suppress the growth of broad-leaved weeds on rice, maize, wheat, and in post-emergence treatments, chlorinated peroxyacetic acid herbicides have been widely utilised in agriculture throughout the world. Because of its chemical and biological stability, 2,4-dichlorophenoxyacetic acid (2,4-D) is the herbicide which is most difficult to break down. It is regarded as a high-toxic contaminant that is carcinogenic and damages both humans and animals.[20]

Receiving waters are contaminated by 2,4-D due to its extensive use and high solubility. High concentrations of this pesticide have frequently been found in drainage water and groundwater, according to reports.[21] 2,4-D has been discovered in shallow water resources, air, human food, and drinking water as a result of its widespread use, water solubility, and low soil adsorption coefficient.[22] Water bodies are contaminated and put in risk by 2,4-D residues left over after its use on farming or from inappropriate disposal. Therefore, it is important to pay attention to the interest in the redemption of 2,4-D by improvements in materials and technology.[23] When it comes to domestic water safety, the purification procedure must be extremely effective and free of secondary pollutants. Therefore, there is an urgent need for an effective way to remove this pesticide from water.[20]

The use of photocatalysts in the photocatalytic degradation process is thought to be a practical and effective way to treat wastewater containing organic contaminants since it has a low operating cost and is effective for organic elimination. Different pre-synthesis extraction techniques used to create Ag nanoparticles were examined for their effects on the photocatalytic degradation of the herbicide dichlorophenoxyacetic acid (2, 4-D).[24]

The main objective of the present study is to synthesis silver nanoparticle and study the photocatalytic degradation efficiency of 2,4-D pollutant. To fulfil the project's objective, the suggested research anticipates the following precise goals- synthesis of AgNPs photocatalyst by co-precipitation method, Study the synthesized nanoparticle's morphological and structural characteristics, 2,4-D degradation by the photocatalytic activity of synthesised Ag nanoparticles and Optimization of various factors using Response Surface Modelling tool.

2. MATERIALS AND METHODS

2.1 Materials and Equipments

All the chemicals and reagents were of analytical grade and were used directly without further purification. Silver nitrate and 2,4 -dichlorophenoxyacetic acid (2,4- D), which is is used as pollutant were obtained from Sigma-Aldrich, India. To prepare the aqueous solutions double distilled water was used. Neem leaves were collected from JSS AHER, Mysuru campus. Magnetic stirrer, Centrifuge, Hot air oven, Muffle furnace and 18-Watt LED light were used at different stages.

2.2 Azadirachta indica (Neem) leaves extract preparation

Fresh neem leaves were gathered from the university grounds in March. After being washed with tap water, the leaves are repeatedly rinsed with double-distilled water to remove the dirt and dust that are present on their surface. To make leaf extract, the washed leaves were dried, precisely weighed, and finely chopped. 500 ml of double-distilled water was added to 20 g of coarsely chopped neem leaves. The mixture was then heated for two hours at 40^0 while being stirred with a magnetic stirrer. The extract was kept for later use, after being filtered using Whatman filter paper and brought to room temperature. This solution was led to the green synthesis of AgNPs.[25,26]

2.3 Synthesis of silver nanoparticle

100 ml of 1 M silver nitrate solution was made using silver nitrate which is depicted in the Figure1. Then 50 ml of neem extract was added to 50 ml of silver nitrate solution. (1:1 ratio). The whole process was carried out in a magnetic stirrer at 600 rpm for 3 hours. Then the solution was kept in dark for a day. The reduction of silver ions is confirmed by the colour change from colourless to brown. Later, this solution is held for centrifugation at 7000 rpm for 10 minutes at -2℃, it is then kept in a hot air oven set to 60^0, retained for cooling at room temperature after drying. Afterwards calcination is done at 400^0.[27,28]

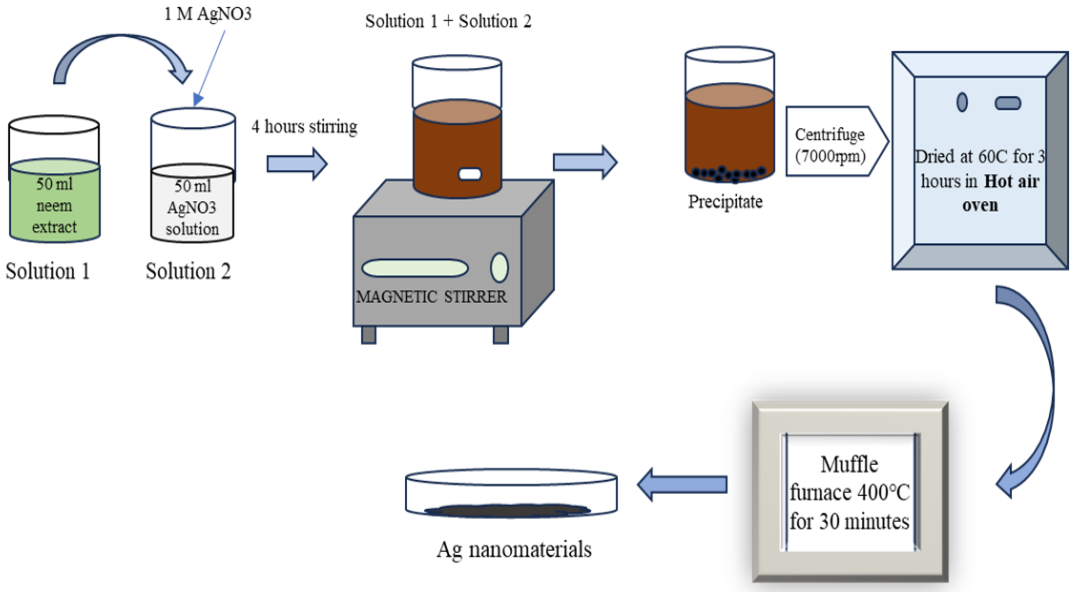

Fig. 1: Preparation of Ag nanomaterial by Co-precipitation method.

2.4 Characterization of the synthesized nanocomposite

The above synthesized photo catalytic nanocomposite was characterized by using many different analytical techniques to analyse the obtained features such as structural elucidation, surface morphology, crystallometry and catalytic activity. The analytical techniques used include Field emission scanning electron microscopy, X- Ray diffraction, Fourier transform infrared spectrometry, Energy dispersive X-ray spectroscopy, UV-Vis's spectroscopy.[29]

2.5 Photodegradation of 2,4-dichlorophenoxyacetic acid (2,4-D)

The organic compound 2,4-Dichlorophenoxyacetic acid, also known as 2,4-D, has the chemical formula $C_8H_6C_{l2}O_3$ is a systemic herbicide. The photocatalytic capability of silver nanoparticles was assessed by evaluating the photodegradation of 2,4-D under both natural and 18-Watt LED light sources. The 2,4-D was photo catalytically degraded by putting 5,10,15 mg of silver nanoparticles in three different containers with concentrations of 5,10 and 15 ppm. The mixture was then maintained in dark condition for 30 minutes to reach in equilibrium. After 30 minutes, the mixture was kept in a magnetic stirrer under artificial light and stirred continuously. Same procedure was done under sunlight also. UV-Vis's spectroscopy was used to measure absorbance at various time intervals.

$$\text{Degradation Efficiency (\%)} = C_o - C_t / C_o \times 100 \quad (1)$$

Where, C_o is the initial concentration of the pollutant, C_t represents the final concentration of the pollutant after the time interval t.[20,30]

Table 1: Ranges of independent variables.

Level	Factors	Upper limit	Lower limit
1	Pollutant's Concentration (ppm)	5	15
2	Amount of Catalyst (mg)	5	15
3	Contact Time (minutes)	30	180

2.6 Experimental design for RSM

RSM has created a few statistical and mathematical techniques to assess the importance of various process parameters. JMP Pro 15 software was used to analyse the reaction, and experimental design calculations were used to anticipate the outcomes. The study focused on three parameters that had two central points and single replicates as outcomes in order to determine the best operating settings for the highest 2,4-D deterioration. The effects of three independent variables—concentration of pollutant, amount of catalyst, and duration period—on the percentage of 2,4-D degradation were examined. The operational levels and ranges of the independent variables evaluated in this study are shown in Table 1. Table 2 displays the results of the nine experimental runs produced by the RSM technique and customised JMP software. In order to examine the effects of independent factors on the experimental study, the response% degradation of 2,4-D was used. To fit the experimental data, a model that correlates the independent variables was developed.

3. RESULTS AND DISCUSSION

3.1 Characterization of Ag Nanoparticle

Morphology of the silver nanoparticle is shown in figure 2. The nanocomposites' microstructures (a) and (b) are enlarged using field emission scanning electron microscopy at X35,000and X80,000, respectively, discloses the morphological structures of the photocatalyst in accordance. Figure (b) clearly depicts the clumping of irregular particles. Ag has achieved granular structures.

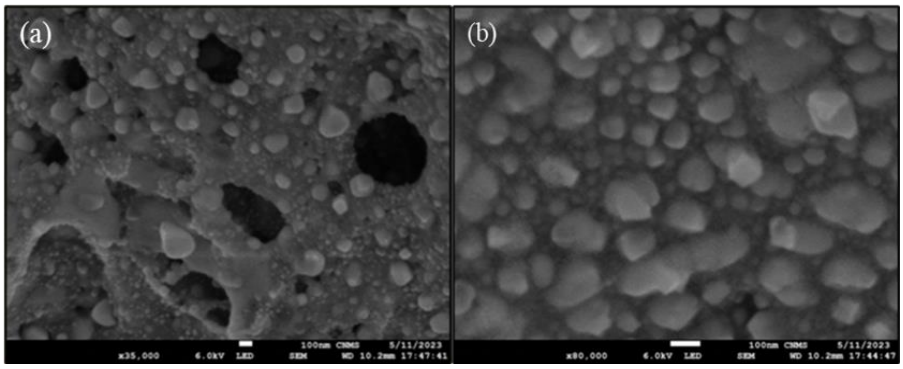

Fig. 2: FESEM representation of silver nanoparticles at different magnifications.

Silver nanoparticle synthesis was verified by EDX analysis. Energy Dispersive-X-ray Spectroscopy was carried out to find out overall compositions of elements in reaction mixture of neem extract and silver nitrate. During the EDX measurement, several areas were targeted, and figure 3 shows the pertinent peaks. N, O, and Ag have peaks that correspond to their respective K, K, and L shell transitions, respectively, in Figure 3, which also includes a data table with the weight percentages of each constituent in the material. The sample comprises 1.01% N, 11.68% O, and 87.31% Ag, with atomic percentages of 4.49%, 45.29%, and 50.22%, respectively.

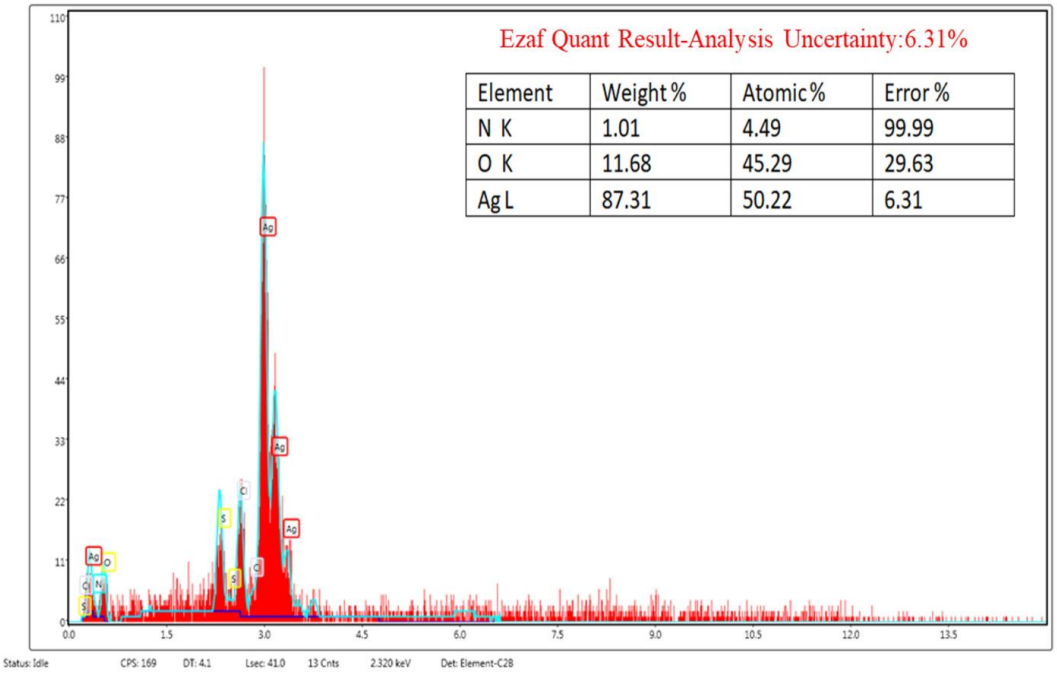

Fig. 3: Elemental composition of AgNPs.

Figure 4 depicts the transmittance versus wave number graph from the FTIR analysis of silver nanoparticles. FTIR image of AgNPs produced by the plant extract displays spectra at 3480, 1384, 1101 and 588 cm^{-1}. A broad peak at 3480 cm^{-1} relates to stretching vibrations of the hydroxyl group. A sharp peak at 1101 and 588 cm1 shows C-C-C and C-Br bending respectively and a small peak at 1384 indicates CH_3CH group.

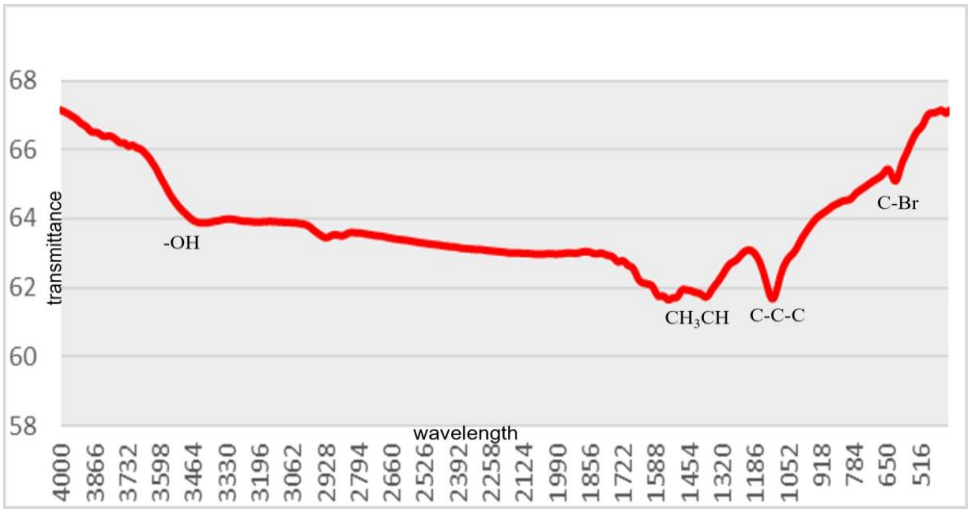

Fig. 4: FTIR Spectra of AgNPs.

The most effective technique for identifying the crystalline structure in a sample using X-Rays of a known wavelength is called X-Ray Diffraction analysis. By using the X-ray diffraction method, the phase identification of the silver nanoparticles was done. The powder XRD measurements in the 2θ range were acquired from 1° to 80°. The peaks occurred at 33.75°, 37.96°, 44.49°, 64.34°, and 77.34°. The sample is silver nanoparticles, according to the diffraction pattern. The mixture's XRD pattern is displayed in figure 5.

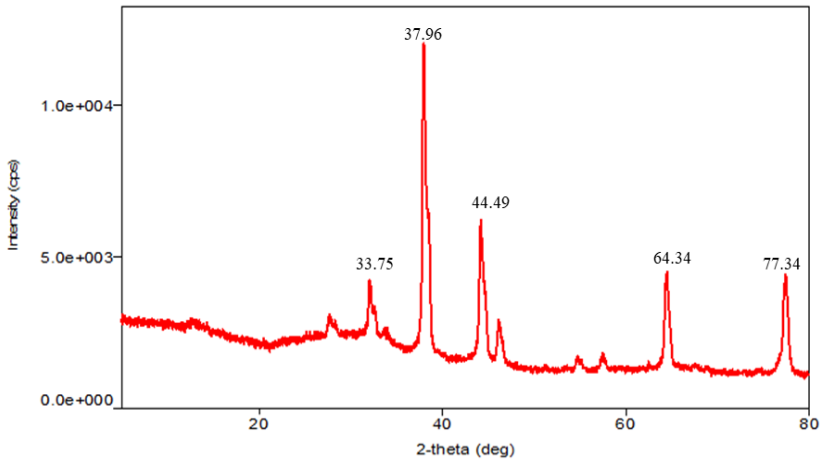

Fig. 5: XRD pattern of silver nanoparticles.

A UV-VIS spectrophotometer was used to estimate the bandgap of the prepared nanocomposite. The UV-Vis spectra were obtained in the 300-800 nm range, as shown in Figure 6 The optical bandgap (Eg) was calculated to be 1.55 eV. Equation (2) is used to determine Eg where h is the Planck constant, υ is the frequency, α is the absorption coefficient, and hυ is the incident photon energy. $(\alpha h\upsilon)2 = A(h\upsilon - Eg)$ ----------(2)

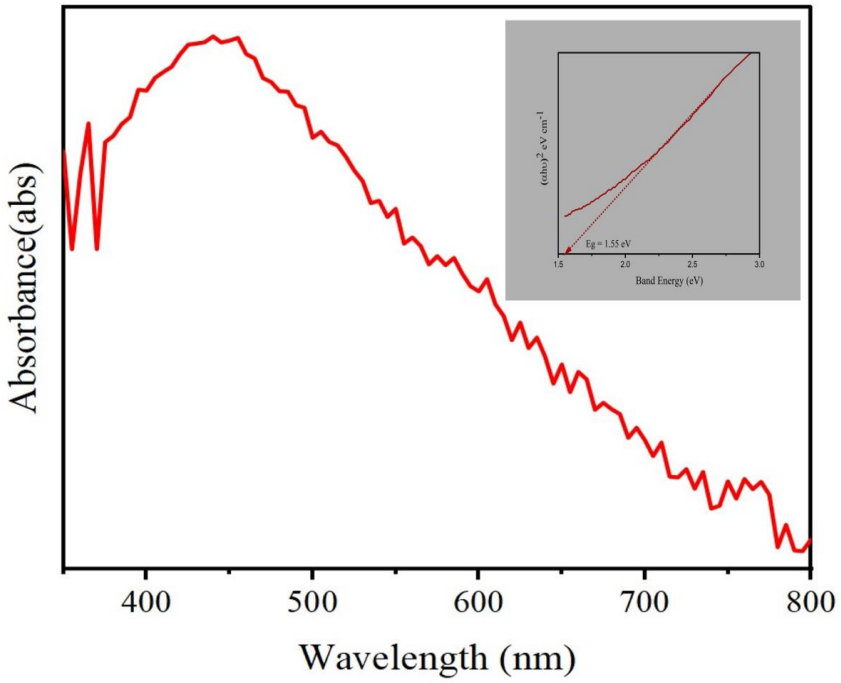

Fig. 6: UV-Vis spectra and band gap.

3.2 Statistical analysis and model development (Response surface modelling for 2,4-Dichlorophenoxyacetic acid degradation)

Response Surface Methodology analysis was carried out for each of the nine trials as they were obtained considering the three independent variables in order to optimise the response factor (pollutant degradation). The initial 2,4-D concentration, the amount of catalyst, and the contact time are all coded as X1, X2, and X3, accordingly. An estimated nine separate experimental trials were produced using the programme mentioned above, and they are shown in Table 2 below. The 2,4-D photo catalytic degradation% was calculated for each trial that was conducted. The relationship between the actual degradation and the anticipated degradation (in both 18-Watt LED light and natural light) is plotted in this study to assess if the used model is relevant or negligible for the pollutant degradation, as illustrated in Figures 7 (a) and (b) below. 2,4-D photo degrades at a rate of 0.98961 R sq. for photo degradation under 18-Watt LED light and 0.99239 R sq. for photo degradation under sunlight. Additionally, the P-value and mean square root error under artificial light are 0.8836 and 0.0304, but they are 0.0516 and 4.5564 in sunlight.

Table 2: Experimental trials created by the RSM method using a custom design.

Trial No.	Pollutant Concentration (ppm)	Amount of Catalyst (mg)	Contact Time(minutes)	%Degradation (18-Watt LED light)	% Degradation (Sunlight)
1	5	5	30	20.0%	24.2%
2	5	5	180	69.6%	73.3%
3	5	15	30	31.5%	35.0%
4	10	10	105	68.2%	72.1%
5	10	10	180	85.8%	90.0%
6	10	15	180	90.2%	93.4%
7	15	5	30	46.0%	51.4%
8	15	5	180	88.0%	91.6%
9	15	15	105	71.1%%	74.3%

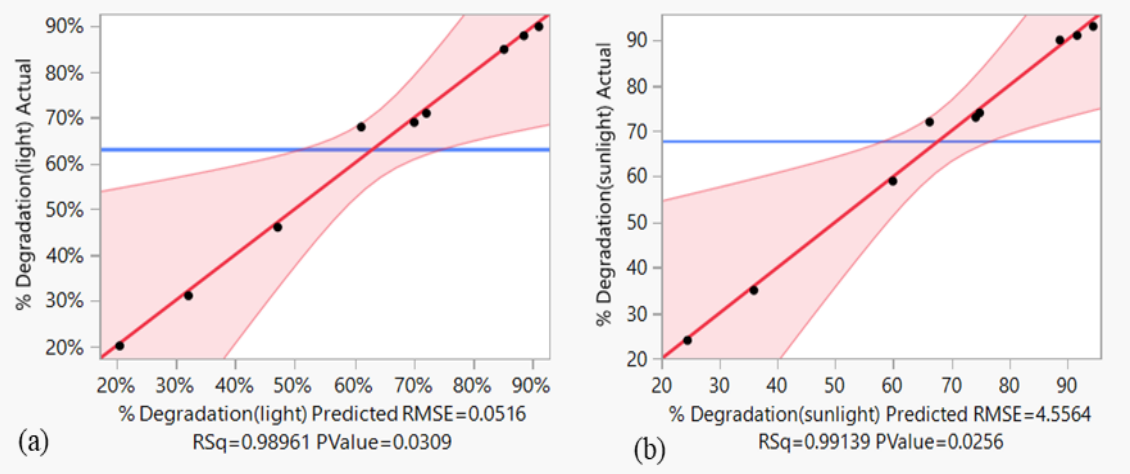

Figure 7: (a) and (b) Graph showing the relationship between actual and anticipated degradation when exposed to 18-Watt LED light and sunlight respectively.

The reliability of the developed model's anticipated results was confirmed using an ANOVA-based study. ANOVA (analysis of variance) is used to obtain the degrees of freedom (DF), sum of squares, mean square, F ratio, and p-value. The results are compiled in Table 3. The sum of the squares from each of the several sources is divided by the relevant degrees of freedom for the model and the error variance to produce the mean square values. The model is further tested in terms of F-value and p-value to confirm its significance. In statistics, a significant model is one with a high F-value (89.4176) and a low P-value (0.0001) in case of artificial light and F-value (74.3583) and a low P-value (0.0001) in case of sunlight. Additionally, the model's fit is confirmed by the coefficient of determination (R^2). As can be shown in Fig. 7(b), the value of the coefficient of determination in this study is R^2=0.99139 under sunlight and 0.98961 under 18-Watt LED light. This shows that 99.10% and 98.90% of the response's variability may be explained by the proposed model. Additionally, the

significant nature of the generated model is demonstrated by the high coefficient of determination (R^2=0.99139).

The relevance of each model parameter (p-value and Log Worth) is shown in Figure 8 here. The Log-Worth is denoted by the notation "-log10 (p-value)", which modifies the p-values to produce a scale that is appropriate for graphing. The reference blue line indicates the two-equivalent -log10(0.01) value. A variable is considered relevant if its Log-Worth value is more than two. Regarding these factors, it was discovered that the contact time had the biggest impact on pollutant's degradation, with logarithms of 2.097 and 0.0079, respectively. The remaining factors, including Pollutant concentration, amount of catalyst, Pollutant concentration*contact period, Catalyst dosage*contact period, and (Pollutant concentration*Catalyst dosage), contain a Log-Worth value.

Table 3: Analysis of variance

(a) 18-Watt LED light.

Source	DF	Sum of Squares	Mean Square	F Ratio
Model	3	0.50311689	0.167706	89.4716
Error	5	0.00937200	0.001874	Prob > F
C. Total	8	0.51248889		<.0001*

(b) Sunlight

Source	DF	Sum of Squares	Mean Square	F Ratio
Model	3	0.49380409	0.164601	74.3583
Error	5	0.01106813	0.002214	Prob > F
C. Total	8	0.50487222		0.0001*

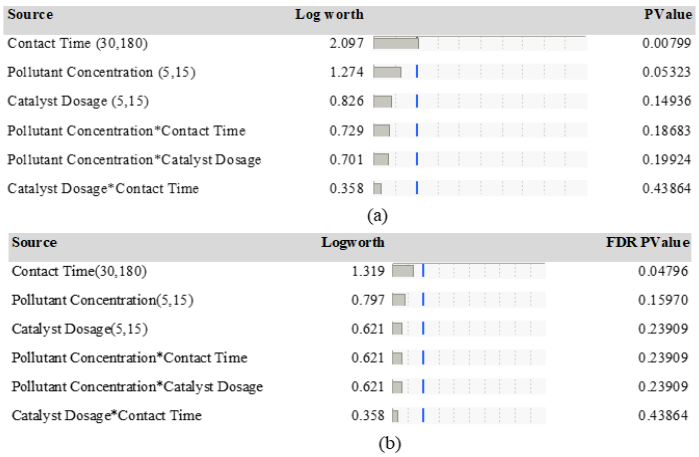

Fig 8: Effect summary revealing the P-value and Log Worth (a) sunlight (b) 18-Watt LED light.

Figure 9 (a) and (b) illustrates residuals vs. anticipated values and residuals, (a) Artificial light and (b) sunlight respectively. A probability distribution of remnants in a range between 0 and 0.06 is shown in Figure 10 (a). Figure 10 (a) displays a stochastic distribution of residues with a range of 0 to 0.06. Figure 10 (b) displays a probability distribution of remnants with a range of -2 and +6.0. The depiction also implies that they are not having a clear pattern or odd structures.it also implies that there are not any clear patterns or odd structures. The illustration of equivalent dispersion below the x-axis adds to the proof that the recommended model is appropriate. Due to the large data points, there is zero residual values and the large points align to create a straight line, the line fit is seen as being more accurate. The constant variance plot of residuals vs. anticipated values was used to test acceptability, while the residuals vs. row number diagram in Fig.9 (a) and (b) was utilized to uncover hidden variables that might impact the response during the experimental activity.

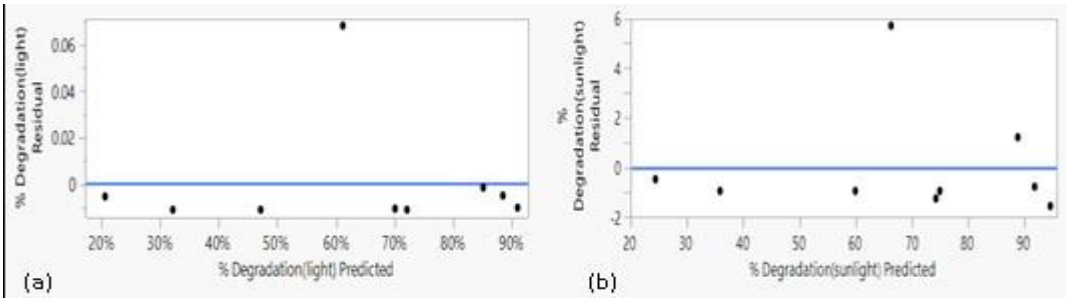

Fig. 9: Graph of degradation residual vs. predicted degradation- (a) Artificial light and (b) sunlight.

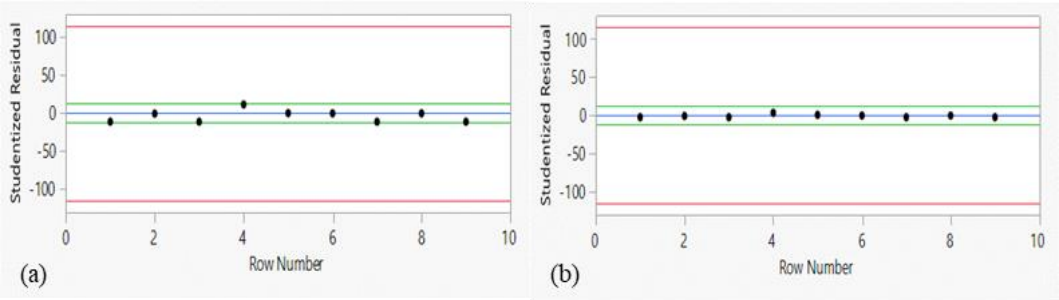

Fig. 10: (a) Graph of residual vs. row number – 18-Watt LED light and (b) sunlight.

To better understand how the independent experimental variable affected the degradation of 2,4-D, JMP was utilised to construct a three-dimensional response surface map. When the pollutant concentration (10 ppm) was at its lowest and the amount of catalyst (15 mg) and duration period (3 hours) were at their highest levels in this investigation, the maximum 2,4-D degradation (93.4%) was seen which was under sunlight. The pollutant concentration (10

ppm) was at its lowest and the amount of catalyst (15 mg) and duration period (3 hours) were at their highest levels under artificial light, and 2,4-D degradation was 90.2%. In case of low concentration of pollutant and duration period and high dose of catalyst under natural light, the 2,4-D degradation was about 35.0%, while it was 31.5% under artificial light. Additionally, the pollutant degradation was lowest when the amount of catalyst, pollutant concentration, and duration period were at their lowest values. The 3D response surface illustrates are shown in the Figure 11, 12 and 13 below. Surface plot in figure 10 shows the impacts of pollutant concentration and catalyst dosage on the breakdown of 2,4-D in both artificial and natural light. The outcomes were plotted in relation to two variables. The results showed that there were substantial interactions between all three parameters. According to the response surface plot in Figure 10, there is a minor rise in the pollutant's percentage of degradation as the pollution concentration rises. The molecules of the photo catalyst and pollutant undergo significant changes in surface charge during this process. According to Fig. 11, the pollutant degradation is significantly influenced by the contact time. In comparison, longer contact duration enhanced pollutant degradation. With the lengthening of the experiment, the degradation percentage significantly increased under both artificial and natural light**.** Figure 12 illustrates how the 2,4-D degradation percentage is significantly impacted by the contact time and pollutant concentration. When the pollutant is exposed to the catalyst for a longer period, the degradation rate increases. The impact of Catalyst dosage vs contact time is depicted in the figure 13. As clearly shown in the Figure 13 as the contact time increases the percentage degradation increase even when the catalyst dosage is less clearly depicting the duration of the advanced oxidation process plays an very important role in this method.

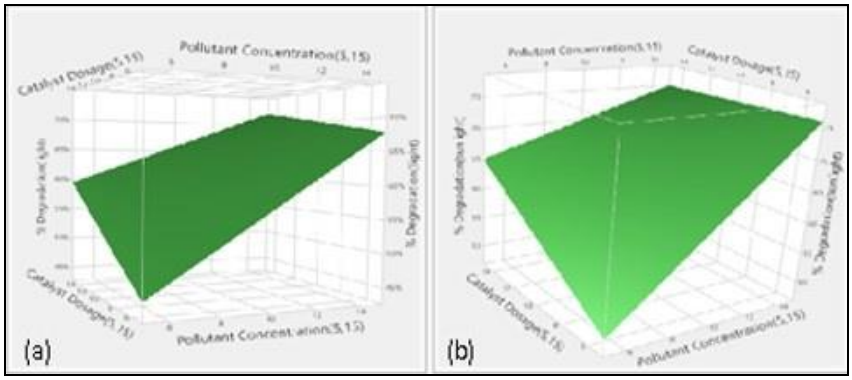

Fig. 11: (a) and (b) An illustration showing the influence of experimental variables on 2,4-D degradation as response surface plots, Catalyst dosage vs. Pollutant concentration under 18-Watt LED light and sunlight respectively.

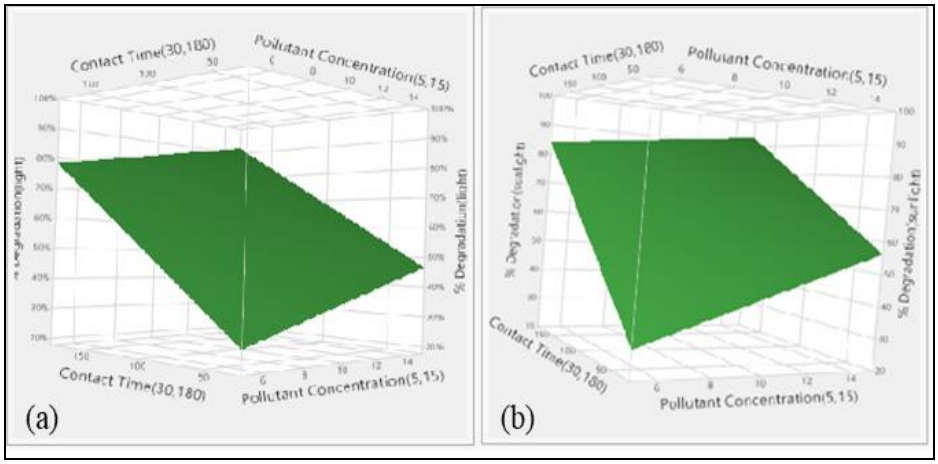

Fig. 12: (a) and (b) An illustration showing the influence of experimental variables on 2,4-D degradation as response surface plots, Pollutant concentration vs. Contact time under 18-Watt LED light and sunlight respectively.

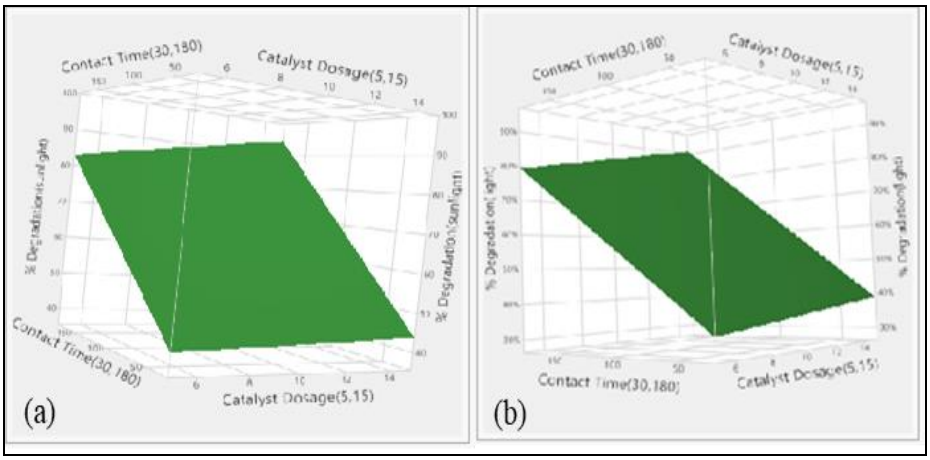

Fig. 13: (a) and (b) An illustration showing the influence of experimental variables on 2,4-D degradation as response surface plots, Catalyst dosage vs. Contact time under 18-Watt LED light and sunlight respectively.

4. CONCLUSION

This study revealed an easy one-pot green production of stable silver nanoparticles using A. indica leaf extract at room temperature. Coprecipitation method was employed for the synthesis of silver nanoparticles which exhibited a remarkable photo catalytic degradation of 2,4-D with 90.20% degradation at 10ppm pollutant concentration, 15mg catalyst dosage under artificial light for 3 hours of contact time and 93.40% degradation at 10 ppm pollutant concentration, 15 mg catalyst dosage under sunlight for 3 hours of contact time. It was discovered that process parameters such the concentration of the neem broth, the ratio of neem extract to $AgNO_3$ solution, and the interaction time, had a significant impact on the

form and size of the nanoparticles produced through bio reduction by neem leaf extract. Furthermore, the relevance of the independent variables like amount of catalyst, pollutant concentration, and duration period was explained by the response surface plots generated by the RSM model. RSM made the optimization process, much efficient and scientific. The results obtained using laboratory experiments and the RSM tool was agreeable with an R sq. value of 0.98961 and P value of 0.0304 under artificial light and R sq. value of 0.99139 and P value of 0.0256 under sunlight. The results demonstrate that the RSM is an excellent tool for enhancing operational mode and a low-cost way for reducing experimentation.

Declaration

Ethics approval

Not applicable.

Consent for publication

Not applicable.

Consent to Participate

Not applicable.

Availability of data and materials

All data generated or analyzed during this study are included in this article [and its supplementary information files].

Competing interests

The authors declare that they have no competing interests.

Funding

Not applicable.

Author contributions

RR executed the experiment and analyzed the obtained results. RR and SSA assisted in the interpretations of the results. NP hypothesized and supervised the study.

ACKNOWLEDGEMENTS

Shenna Sreejan Anuvrinda acknowledges the JSS Academy of Higher Education and Research, Mysuru, provided a laboratory facility to the authors.

REFERENCES

1. Sunkar S, Nachiyar CV. Biogenesis of antibacterial silver nanoparticles using the endophytic bacterium Bacillus cereus isolated from Garcinia xanthochymus. Asian Pac J Trop Biomed, 2012; 2(12): 953–9.
2. Arumai Selvan D, Mahendiran D, Senthil Kumar R, KalilurRahiman A. Garlic, green tea and turmeric extracts-mediated green synthesis of silver nanoparticles: Phytochemical, antioxidant and in vitro cytotoxicity studies. J Photochem Photobiol B., Mar. 1, 2018; 180: 243–52.
3. Khalil MMH, Ismail EH, El-Baghdady KZ, Mohamed D. Green synthesis of silver nanoparticles using olive leaf extract and its antibacterial activity. Arabian Journal of Chemistry, Dec. 1, 2014; 7(6): 1131–9.
4. Gomathi M, Rajkumar PV, Prakasam A, Ravichandran K. Green synthesis of silver nanoparticles using Datura stramonium leaf extract and assessment of their antibacterial activity. Resource-Efficient Technologies, Sep. 2017; 3(3): 280–4.
5. Kumar B, Smita K, Cumbal L, Debut A. Green synthesis of silver nanoparticles using Andean blackberry fruit extract. Saudi J Biol Sci., Jan. 1, 2017; 24(1): 45–50.
6. Abbas S, Nasreen S, Haroon A, Ashraf MA. Synhesis of Silver and Copper Nanoparticles from Plants and Application as Adsorbents for Naphthalene decontamination. Saudi J Biol Sci., Apr. 1, 2020; 27(4): 1016–23.
7. Guilger-Casagrande M, Lima R de. Synthesis of Silver Nanoparticles Mediated by Fungi: A Review. Vol. 7, Frontiers in Bioengineering and Biotechnology. Frontiers Media S.A., 2019.
8. Bar H, Bhui DK, Sahoo GP, Sarkar P, De SP, Misra A. Green synthesis of silver nanoparticles using latex of Jatropha curcas. Colloids Surf APhysicochem Eng Asp., May 1, 2009; 339(1–3): 134–9.
9. Mahdieh M, Zolanvari A, Azimee AS, Mahdieh M. Green biosynthesis of silver nanoparticles by Spirulina platensis. Scientia Iranica, 2012; 19(3): 926–9.
10. Edison TJI, Sethuraman MG. Instant green synthesis of silver nanoparticles using Terminalia chebula fruit extract and evaluation of their catalytic activity on reduction of methylene blue. Process Biochemistry, Sep. 2012; 47(9): 1351–7.
11. Kahrilas GA, Wally LM, Fredrick SJ, Hiskey M, Prieto AL, Owens JE. Microwave-assisted green synthesis of silver nanoparticles using orange peel extract. ACS Sustain Chem Eng., Mar. 3, 2014; 2(3): 367–76.

12. Kumar DA, Palanichamy V, Roopan SM. Green synthesis of silver nanoparticles using Alternanthera dentata leaf extract at room temperature and their antimicrobial activity. Spectrochim Acta A Mol BiomolSpectrosc, Jun. 5, 2014; 127: 168–71.
13. Pawar AA, Sahoo J, Verma A, Alswieleh AM, Lodh A, Raut R, et al. Azadirachta indica -Derived Silver Nanoparticle Synthesis and Its Antimicrobial Applications. J Nanomater, 2022; 2022.
14. Ashokkumar S, Ravi S, Velmurugan S. Green synthesis of silver nanoparticles from Gloriosa superba L. leaf extract and their catalytic activity. Vol. 115, Spectrochimica Acta - Part A: Molecular and Biomolecular Spectroscopy. Elsevier B.V., 2013; 388–92.
15. Ravichandran V, Vasanthi S, Shalini S, Ali Shah SA, Harish R. Green synthesis of silver nanoparticles using Atrocarpusaltilis leaf extract and the study of their antimicrobial and antioxidant activity. Mater Lett., Oct. 1, 2016; 180: 264–7.
16. Ahmed S, Saifullah, Ahmad M, Swami BL, Ikram S. Green synthesis of silver nanoparticles using Azadirachta indica aqueous leaf extract. J Radiat Res Appl Sci., Jan. 2016; 9(1): 1–7.
17. Namratha N, Monica P V. Synthesis of silver Nanoparticles using Azadirachta indica (Neem) extract and usage in water purification [Internet]. Vol. 3, Asian J. Pharm. Tech., 2013. Available from: www.asianpharmaonline.org
18. Alsammarraie FK, Wang W, Zhou P, Mustapha A, Lin M. Green synthesis of silver nanoparticles using turmeric extracts and investigation of their antibacterial activities. Colloids Surf B Biointerfaces, Nov. 1, 2018; 171: 398–405.
19. Sánchez OA, Rodríguez JL, Barrera-Andrade JM, Borja-Urby R, Valenzuela MA. High performance of Ag/$BiVO_4$ photocatalyst for 2,4-Dichlorophenoxyacetic acid degradation under visible light. Appl Catal A Gen, Jun. 25, 2020; 600.
20. Tang Y, Luo S, Teng Y, Liu C, Xu X, Zhang X, et al. Efficient removal of herbicide 2,4-dichlorophenoxyacetic acid from water using Ag/reduced graphene oxide co-decorated TiO_2 nanotube arrays. J Hazard Mater, Nov. 30, 2012; 241–242:323–30.
21. Jaafarzadeh N, Ghanbari F, Ahmadi M. Catalytic degradation of 2,4-dichlorophenoxyacetic acid (2,4-D) by nano-Fe_2O_3 activated peroxymonosulfate: Influential factors and mechanism determination. Chemosphere, Feb. 1, 2017; 169: 568–76.
22. Golshan M, Kakavandi B, Ahmadi M, Azizi M. Photocatalytic activation of peroxymonosulfate by TiO_2 anchored on cupper ferrite (TiO_2@$CuFe_2O_4$) into 2,4-D

degradation: Process feasibility, mechanism and pathway. J Hazard Mater, Oct. 5, 2018; 359: 325–37.

23. S S, Nagashree KL, Maiyalagan T, Keerthiga G. Photocatalytic degradation of 2,4-dichlorophenoxyacetic acid - A comparative study in hydrothermal TiO_2 and commercial TiO_2. Appl Surf Sci., Aug. 15, 2018; 449: 371–9.
24. Kamarudin NS, Jusoh R, Sukor NF, Jalil AA, Setiabudi HD. Intensified photocatalytic degradation of 2, 4–dicholorophenoxyacetic acid using size-controlled silver nanoparticles: Effect of pre-synthesis extraction. Advanced Powder Technology, Aug. 1, 2020; 31(8): 3381–94.
25. Roy P, Das B, Mohanty A, Mohapatra S. Green synthesis of silver nanoparticles using azadirachta indica leaf extract and its antimicrobial study. Applied Nanoscience (Switzerland), Nov. 1, 2017; 7(8): 843–50.
26. Giri PK. International Conference on Advanced Nanomaterials and Nanotechnology : ICANN-2009 ; Guwahati, India ; 9-11 December 2009. American Institute of Physics, 2010; 440.
27. Verma A, Mehata MS. Controllable synthesis of silver nanoparticles using Neem leaves and their antimicrobial activity. J Radiat Res Appl Sci., Jan. 2016; 9(1): 109–15.
28. Mankad M, Patil G, Patel D, Patel P, Patel A. Comparative studies of sunlight mediated green synthesis of silver nanoparaticles from Azadirachta indica leaf extract and its antibacterial effect on Xanthomonas oryzaepv. oryzae. Arabian Journal of Chemistry, Jan. 1, 2020; 13(1): 2865–72.
29. Tripathy A, Raichur AM, Chandrasekaran N, Prathna TC, Mukherjee A. Process variables in biomimetic synthesis of silver nanoparticles by aqueous extract of Azadirachta indica (Neem) leaves. Journal of Nanoparticle Research, Jan. 2010; 12(1): 237–46.
30. Kamarudin NS, Jusoh R, Jalil AA, Setiabudi HD, Sukor NF. Synthesis of silver nanoparticles in green binary solvent for degradation of 2,4-D herbicide: Optimization and kinetic studies. Chemical Engineering Research and Design, Jul. 1, 2020; 15(9): 300–14.